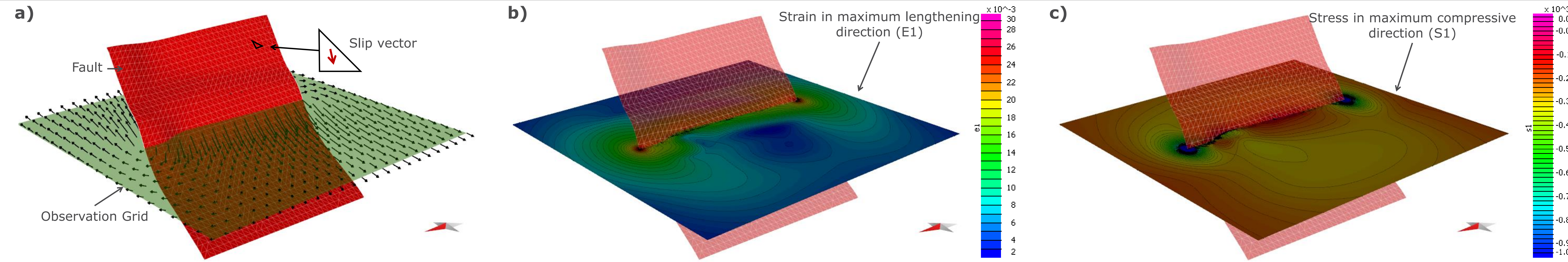


# Geological applications for the new Fault Response Modelling tool in Move™

MACAULAY, E., BROICHHAUSEN, H., ELLIS, J., VAUGHAN, A. and DAVIS, T.  
 Midland Valley Exploration Ltd, 2 West Regent Street, Glasgow G2 1RW. E-mail: [emac@mve.com](mailto:emac@mve.com)  
[www.mve.com](http://www.mve.com)

## Introduction

When a fault slips, subsequent displacement, strain and stress can be analytically calculated using elastic dislocation theory (Figure 1). An analytical solution for triangular dislocation has been implemented in Move in the form of the easy-to-use Fault Response Modelling tool. Fault Response Modelling, combined with the structural modelling and restoration functions of Move, offers unparalleled insights into the effects of faulting across different time intervals and has many potential applications in earthquake prediction, hydrocarbon exploration and the mining industry. This range of possible applications is demonstrated by applying new workflows to four different case studies.



**Figure 1:** Illustration showing the use of Fault Response Modelling to calculate displacements, strain and stress following normal slip on a fault. a) Displacement of points on the observation grid (black arrows) calculated by superimposing displacements induced by slip on each fault triangle. b) Strain is calculated from the displacements; magnitudes and orientations of the strain tensor can be visualized. c) Stresses induced by faulting are calculated from strain using Hooke's Law. Regional stress can be incorporated.



## Case Study 1: Earthquake-induced stress modelling

### Background

Slip on a fault alters the surrounding stress field, and can cause nearby faults to fail, causing aftershocks (King et al., 1994).

### Objective

Model the slip event that led to the Nura earthquake in Kyrgyzstan in 2008 (Teshbaeva et al., 2014); compare predicted displacements and stress changes to satellite data and aftershock distribution.

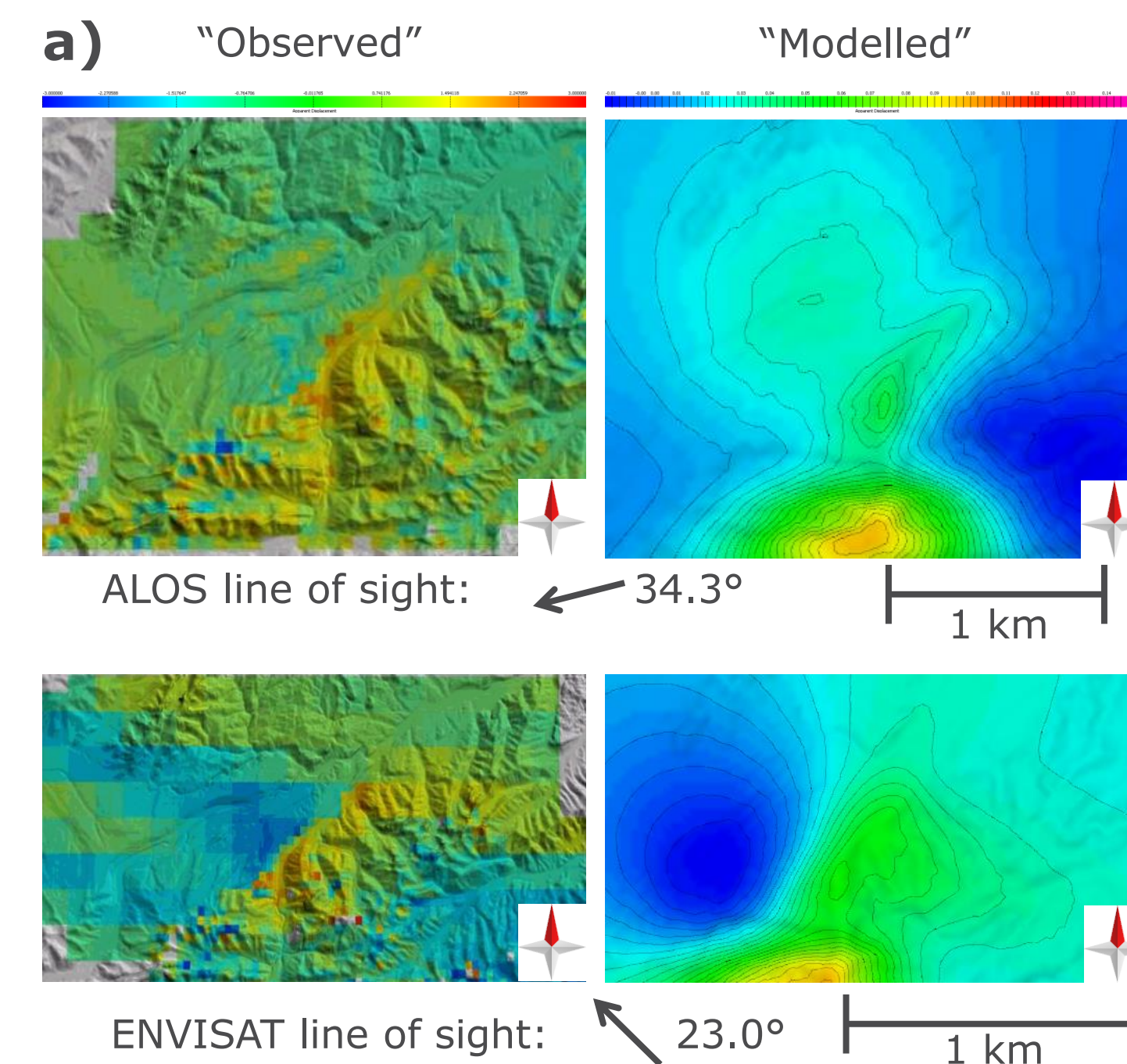


**Figure 2:** a) Similar apparent displacements from "observed" satellite data and "modelled" using Fault Response Modelling. b) Modelled isosurface representing area around faults with Coulomb stress changes of >0.17 MPa on optimally orientated planes following the modelled earthquake (grey mesh). Distribution of observed aftershocks (black points) reproduced reasonably well by modelling, except along strike to the northeast.

**References**  
 King, G. C., Stein, R. S., & Lin, J. (1994). Static stress changes and the triggering of earthquakes. *Bulletin of the Seismological Society of America*, 84(3), 935-953.  
 Teshbaeva, K., Sudhaus, H., Echter, H., Schurr, B., & Roessner, S. (2014). Strain partitioning at the eastern Pamir-Alai revealed through SAR data analysis of the 2008 Nura earthquake. *Geophysical Journal International*, ggu158.

## Case Study 2: Fracture prediction in a hydrocarbon reservoir

### Background

Fracture systems influence porosity, permeability and the connectivity of hydrocarbon reservoirs.

### Objective

Use Fault Response Modelling to predict the orientations of fractures in a pop-up block within the La Concepcion oilfield in the north-western Maracaibo Basin of Venezuela. Compare to observed fractures to assess whether they are controlled by dip-slip faulting.

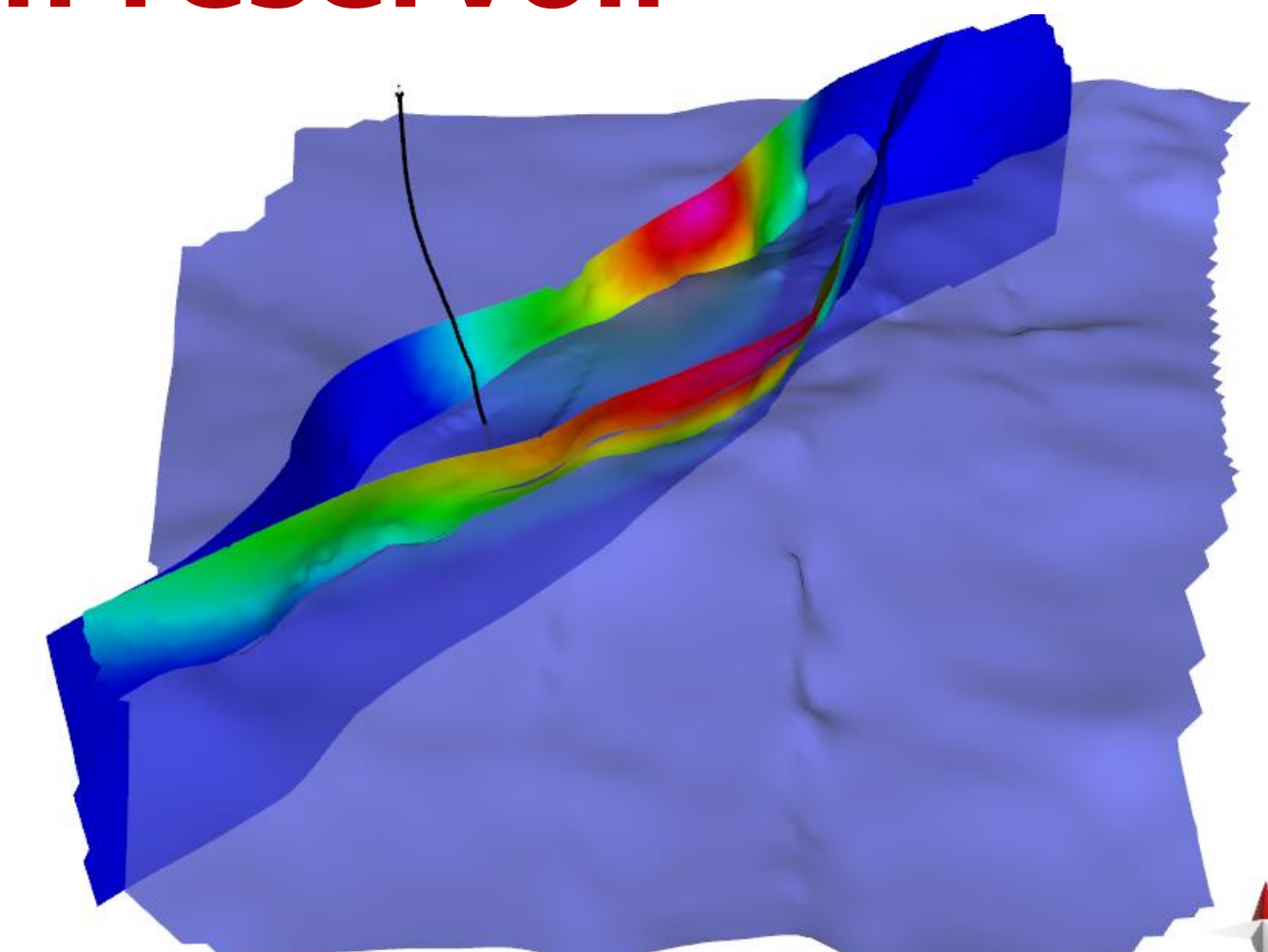


**Figure 3:** Slip gradients on the faults bounding the pop-up block were based on the displacement of the Maraca horizon (blue) and were calculated using the Allan Mapper tool in Move. Black line shows well location.

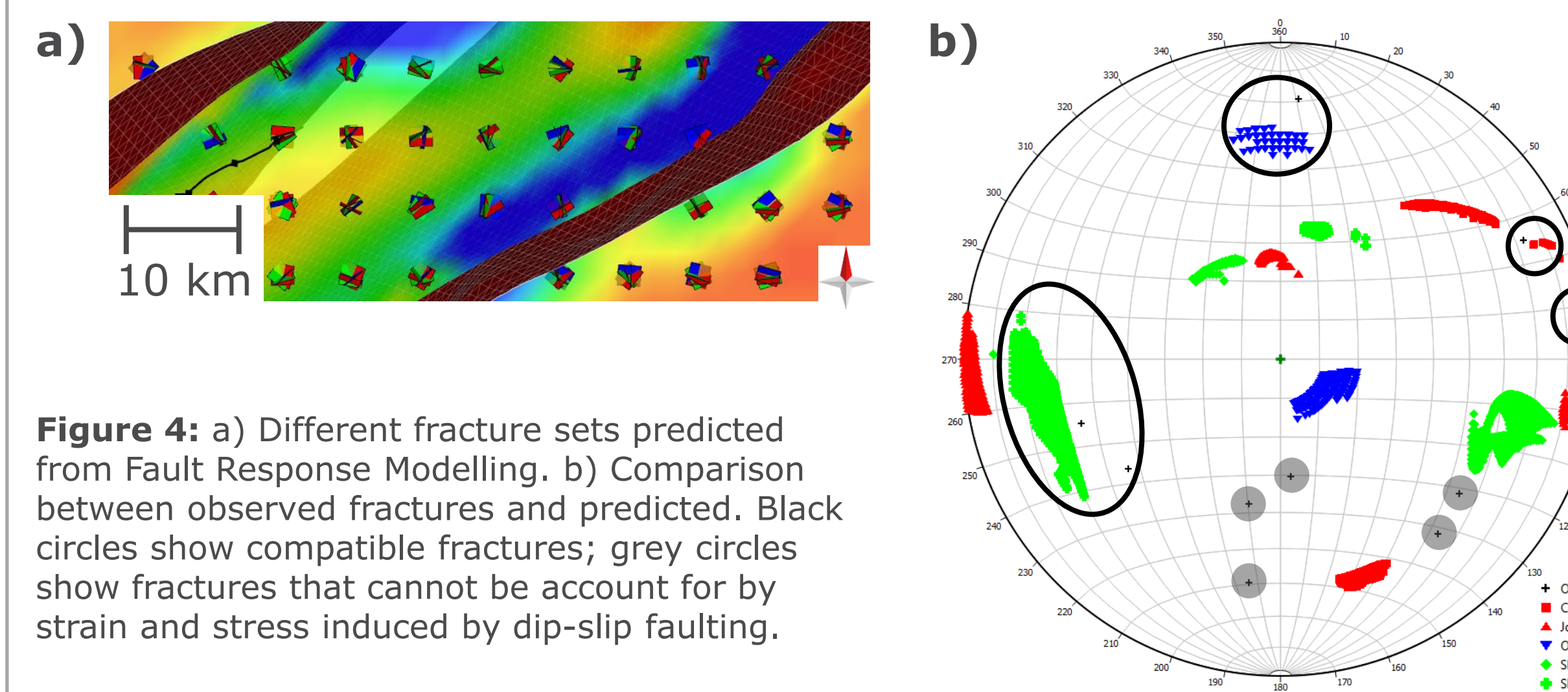


**Figure 4:** a) Different fracture sets predicted from Fault Response Modelling. b) Comparison between observed fractures and predicted. Black circles show compatible fractures; grey circles show fractures that cannot be accounted for by strain and stress induced by dip-slip faulting.

**References**  
 Porras, J. S., et al. Petrobras Energía, S. A. (2007, April). Fractured Basement: New Exploratory Target in La Concepción Field, Western Venezuela. In *AAPG Annual Convention, Search and Discovery Article 10140*.

## Case Study 3: Ore body formation controlled by fault-related damage

### Background

Fracturing in damage zones around active faults often exerts first-order controls on fluidization and mineralization (Micklewaite and Cox, 2004).

### Objective

Use proxies for fracture intensity, calculated by the Fault Response Modelling tool, to predict gold mineralization in the northern Carlin Trend in Nevada, USA (Micklewaite, 2011).

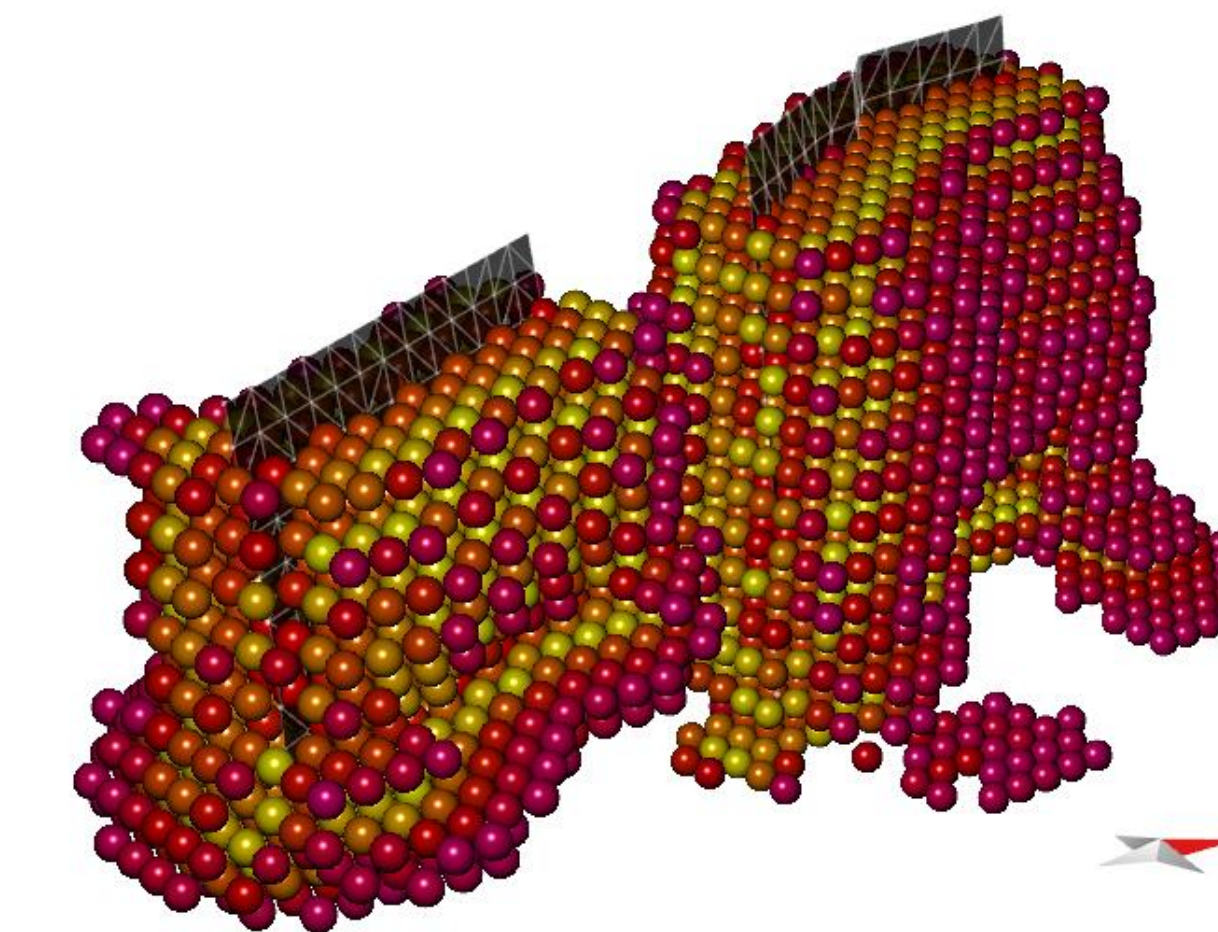


**Figure 5:** Coulomb stress change on joints (orientation based on strain tensor); highest Coulomb stress change around faults.

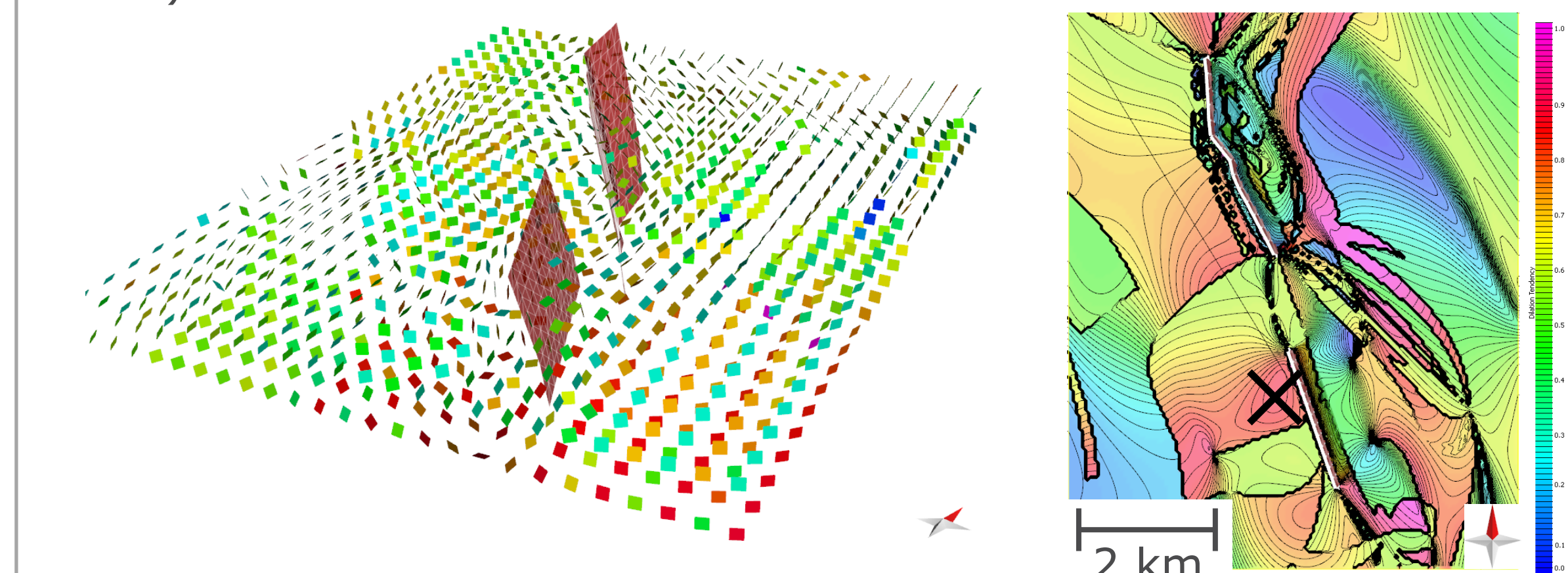


**Figure 6:** Joints colour coded for dilation tendency associated with fault-induced stresses (left); dilation tendency colour mapped and contoured onto the observation grid (right). High dilation tendency near fault coincides with high Coulomb stress change and identifies a potential target (indicated with black cross).

**References**  
 Micklethwaite, S., & Cox, S. F. (2004). Fault-segment rupture, aftershock-zone fluid flow, and mineralization. *Geology*, 32(9).  
 Micklethwaite, S. (2011). Fault-induced damage controlling the formation of Carlin-type ore deposits.

## Case Study 4: Geomechanical forward modelling of faults

### Background

Forward modelling is a powerful validation technique; if an interpretation cannot be reproduced it cannot be correct. Fault Response Modelling can geomechanically forward model fault-related deformation whilst considering the mechanical properties of the rock (including any spatial variations).

### Objective

Geomechanically validate an interpretation of a listric normal fault by forward modelling the fault-related deformation. In particular, determine whether it is geomechanically feasible that hangingwall rollover could extend 15 km laterally from the fault.

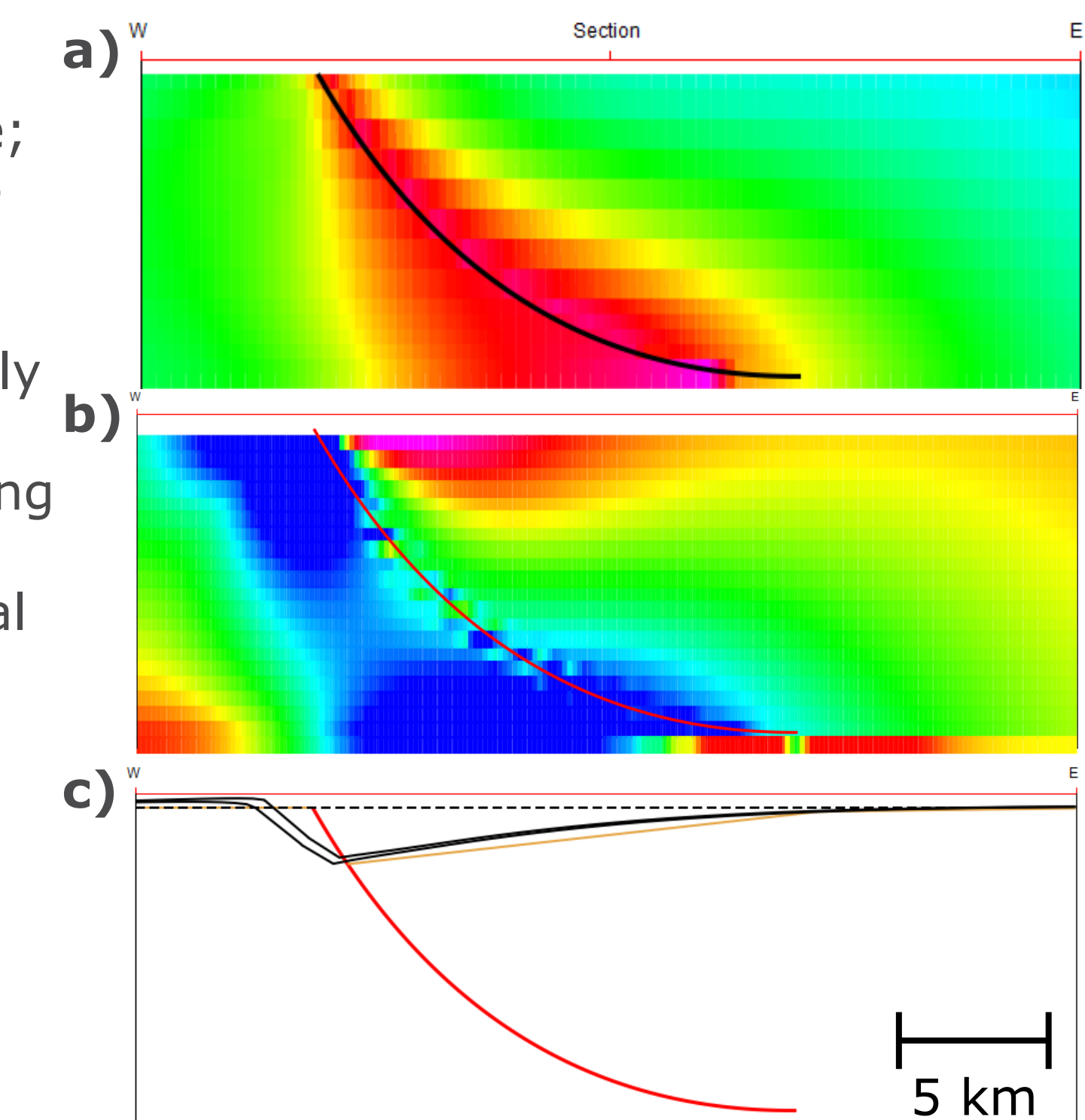


**Figure 7:** a) Total displacement around a modelled listric normal fault. b) Magnitude of S1 from the fault-induced stress. c) Comparison between interpretation (brown) and geomechanically forward modelled horizons (black) for Poisson's ratio of 0.25 (lower line) and 0.4 (upper line). d) 3D view showing displacement on the pre-slip surface.

